Journal of Oceanology and Limnology
Vol. 37 No. 5, P. 1542-1554, 2019
https://doi.org/10.1007/s00343-019-8079-z

Gaussian decomposition and component pigment spectral analysis of phytoplankton absorption spectra*

YE Huping[1, 2, 3, 4], ZHANG Bing[2], LIAO Xiaohan[1], LI Tongji[3], SHEN Qian[2], ZHANG Fangfang[2], ZHU Jianhua[3, **], LI Junsheng[2, **]

[1] *State Key Laboratory of Resources and Environmental Information System*, *Institute of Geographic Sciences and Natural Resources Research*, *Chinese Academy of Sciences*, *Beijing 100101*, *China*

[2] *Institute of Remote Sensing and Digital Earth*, *Chinese Academy of Sciences*, *Beijing 100094*, *China*

[3] *National Ocean Technology Center*, *Tianjin 300112*, *China*

[4] *China-Sri Lanka Joint Research and Demonstration Center for Water Technology*, *Chinese Academy of Sciences*, *Beijing 100085*, *China*

Received Apr. 28, 2018; accepted in principle Oct. 29, 2018; accepted for publication Jan. 16, 2019

Abstract The absorption spectrum of phytoplankton is an important bio-optical parameter for ocean color hyperspectral remote sensing; its magnitude and shape can be affected considerably by pigment composition and concentration. We conducted Gaussian decomposition to the absorption spectra of phytoplankton pigment and studied the spectral components of the phytoplankton, in which the package effect was investigated using pigment concentration data and phytoplankton absorption spectra. The decomposition results were compared with the corresponding concentrations of the five main pigment groups (chlorophylls *a*, *b*, and *c*, photo-synthetic carotenoids (PSC), and photo-protective carotenoids (PPC)). The results indicate that the majority of residual errors in the Gaussian decomposition are <0.001 m^{-1}, and R^2 of the power regression between characteristic bands and HPLC pigment concentrations (except for chlorophyll *b*) was 0.65 or greater for surface water samples at autumn cruise. In addition, we determined a strong predictive capability for chlorophylls *a*, *c*, PPC, and PSC. We also tested the estimation of pigment concentrations from the empirical specific absorption coefficient of pigment composition. The empirical decomposition showed that the Ficek model was the closest to the original spectra with the smallest residual errors. The pigment decomposition results and HPLC measurements of pigment concentration are in a high consistency as the scatter plots are distributed largely near the 1:1 line in spite of prominent seasonal variations. The Woźniak model showed a better fit than the Ficek model for Chl *a*, and the median relative error was small. The pigment component information estimated from the phytoplankton absorption spectra can help better remote sensing of hyperspectral ocean color that related to the changes in phytoplankton communities and varieties.

Keyword: phytoplankton absorption spectrum; pigment concentration; Gaussian decomposition

1 INTRODUCTION

The phytoplankton absorption coefficient ($a_{ph}(\lambda)$) is an important parameter used in various applications (Chase et al., 2013, 2017; Werdell et al., 2014), such as pigment biomass remote sensing, light attenuation in the ocean, upper ocean carbon fixation, and mixed layer heating. It can be obtained by in situ measurement of water samples (Pegau et al., 2003) or inversion from hyperspectral ocean color remote sensing (Lee and Carder, 2004). Generally, the pattern of the

* Supported by the National Natural Science Foundation of China (Nos. 91638201, 41276184, 41771388 41471308, 41571361, 41701402), the Strategic Priority Research Program of Chinese Academy of Sciences (No. XDA2003030201), the National Key Research and Development Program of China (Nos. 2017YFB0503005, 2016YFC1400903, 2016YFB0501502), the High Resolution Earth Observation Systems of National Science and Technology Major Projects (No. 41-Y20A31-9003-15/17), the China-Sri Lanka Joint Research and Demonstration Center for Water Technology, and the State Development and Reform Commission's Special Financial Projects (No. 2017ST000602)
** Corresponding authors: besmile@263.net; lijs@radi.ac.cn

absorption spectrum is affected by chlorophyll *a* concentration, algal species, and the algal cell size, and the absorption spectrum varies with the pigment composition changes in terms of the relative proportion of accessory pigments, namely chlorophyll *b* and *c*, as well as a variety of carotenoids and phycobiliproteins). Each pigment element features a specific absorption spectrum (Bricaud et al., 2007). In addition, pigments do not distribute evenly in phytoplankton cells but are located in small "packages" (chlorophyll), while chlorophyll exhibits a relatively homogenous distribution of pigments in extraction solvent. This is defined as the "package effect". The package effect and the proportion of accessory pigment compositions are two major factors influencing the changes in pattern and magnitude of the chlorophyll-specific absorption coefficient of phytoplankton ($a^*_{ph}(\lambda)$) (Morel and Bricaud, 1981; Sathyendranath et al., 1987; Le et al., 2009; Ferreira et al., 2017). The package effect cannot be directly measured but can be described according to phytoplankton particle size and pigment concentration in cells. Researchers have previously described the population structure and particle size of plankton through pigment composition (Bricaud et al., 2004). In addition, empirical models of particle size using chlorophyll *a* concentration have been used to correct for the package effect, as in the marine algorithm constructed by Woźniak et al. (2000), the Antarctic waters algorithm constructed by Ferreira et al. (2017), and the Baltic Sea algorithm proposed by Ficek et al. (2004).

There are many types of phytoplankton pigments, generally in five main categories: chlorophyll *a* (Chl *a*), chlorophyll *b* (Chl *b*), chlorophyll *c* (Chl *c*), photosynthetic carotenoids (PSC), and photoprotective carotenoids (PPC) (Bidigare et al., 1990; Woźniak et al., 2000; Ficek et al., 2004; Chase et al., 2013, 2017; Wang et al., 2018). The absorption spectra of photosynthetic organisms from 400 to 700 nm are characterized by a continuous envelope curve, reflecting energy transfer in strong coupling among pigment molecules. The continuity of the spectrum makes it very difficult to separate the contribution from each pigment to the total absorbance unless the absorption spectrum is decomposed appropriately. There are many methods of decomposition of phytoplankton absorption spectrum into the five major pigment components, such as the fourth derivative method (Bidigare et al., 1989; Vijayan et al., 2014), multiple linear regression (Bidigare et al., 1990), Gaussian characteristic band decomposition (Woźniak et al., 2000; Ficek et al., 2004), and the neural network multilayer perceptron model (Bricaud et al., 2007; Zhou et al., 2010), etc. The fourth derivative method is unable to discriminate a pigment of wide absorption bands. The multilayer perceptron modeling uses the nonlinear function relationships of neural networks and the key to the model establishment is choosing representative training samples, which requires relatively complex programming and debugging. The multiple linear regression and Gaussian characteristic band decomposition are limited to reach high accuracy of retrieval by the package effect.

To analyze the effect of accessory pigments on the measurement of phytoplankton absorption, we should consider the contribution of each pigment to the absorption spectra in unpackaged conditions, namely in vivo pigment absorption spectra. Hoepffner and Sathyendranath (1991) proposed a method in which an absorption spectrum can be segmented into 13 Gaussian absorption bands that can be fitted to curves and combined with HPLC (high performance liquid chromatography) measurements of the concentration of each pigment to construct a linear relationship between pigment concentration and Gaussian band amplitude. Bricaud et al. (2004), Chase et al. (2013, 2017), Wang et al. (2018), and others used similar methods. The multiple linear regression assumes that an in vivo specific absorption coefficient obtained from known measurements of extracted pigments can represent the unknown complex pigment-protein specific absorption coefficients, and linearly fits them to absorption spectra in unpackaged conditions. Typical examples include the models of Bidigare et al. (1990), Woźniak et al. (2000), and Ficek et al. (2004) for the five major pigment components and the Gaussian model of Hoepffner and Sathyendranath (1991) for the synthesis of four pigment components. The Gaussian decomposition of phytoplankton absorption spectra and pigment spectral component analysis are often applied in oceanic and eutrophic offshore waters but less applied in turbid offshore waters. Therefore, the suitability of the decomposition model for offshore waters and their seasonal variability in China should be investigated.

This study corrects the package effect of phytoplankton absorption spectra in the Yellow/East China Sea using pigment concentrations obtained from HPLC measurements, in which the corrected

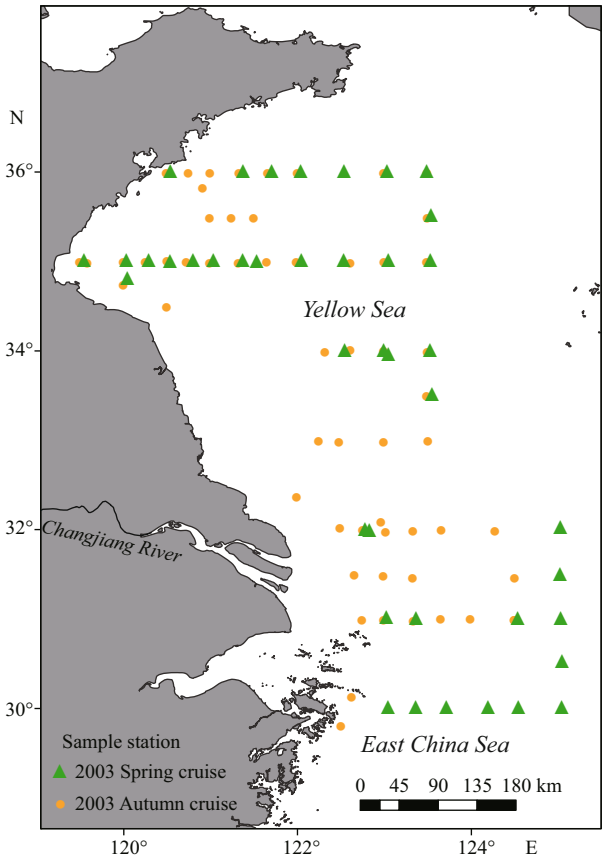

Fig.1 Sample stations of spring and autumn cruises in 2003 (28 stations overlapped)

phytoplankton absorption spectra can be avoided of being affected by the cell size and pigment packaging largely. The absorption spectra are decomposed in Gaussian characteristic bands or pigment compositions. The results are compared with data measured by HPLC, and the changes by different seasons are analyzed in the study area.

2 DATA AND METHOD

2.1 Data collection

Pigment composition and absorption spectra datasets were collected in two Yellow/East China Sea cruises in April 2003 (spring) and September 2003 (autumn) (Fig.1). In the spring cruise, water samples were collected from 10-m and 20-m (or 15-m due to depth limit) water layers in 41 stations. In the autumn cruise, water samples were collected from 0-m and 5-m water layers in 58 stations. From both cruises, 167 sets of pigment composition and absorption spectra are well matched.

The absorption parameter (a_{ph}) of each water sample is measured using the quantitative filter technique (QFT) (Mitchell, 1990). To determine the $a_{ph}(\lambda)$, water samples are first filtered through Millipore membrane filters of 0.2 μm pore to remove particulate material. The null correction of $a_g(\lambda)$ absorption values is selected by setting the mean values from 690 to 700 nm to zero (Pegau et al., 2003; Zhu, 2003a). Samples for phytoplankton pigment analysis are collected, filtered, and preserved in the same manner as in the QFT analysis. The methanol extraction is used to remove the algal component and then $a_{ph}(\lambda)$ can be acquired by subtracting non-pigment particles $a_d(\lambda)$ from the absorption coefficients of total particles $a_p(\lambda)$ (Zhu, 2003a). The concentrations of component pigments in water samples are analyzed in HPLC as described by Zhu (2003b) and Zhu et al. (2017), in which the measurement system is combined with a C18 (ODS) chromatography column for reverse-phase chromatography in a ternary gradient. Briefly, samples are extracted in 3 mL 100% HPLC grade acetone ($V_{Extracted}$) at 0°C in darkness for 24 h; 1 mL of the final extract is mixed with 0.3 mL HPLC grade water and injected into a Waters 600E HPLC system equipped with a 996-photodiode array detector (PDA). A ternary solvent system is employed for HPLC pigment analysis. According to the chromatographic data of pigment standards, the absorbance spectra of different pigments in the wavelength range of 350 nm to 800 nm ($OD_{HPLC,i}(\lambda)$) are measured. The absorption coefficient of each pigment of each sample is calculated by Eq.1 below. The summation of total absorption coefficients of all pigments in each sample resulted in the pigment absorption coefficient ($a_{HPLC,\varphi}(\lambda)$) of a particular sample.

$$a_{HPLC,\varphi}(\lambda)=\sum_{i}^{n}2.303\times OD_{HPLC,i}\times\frac{V_{Extracted}}{l\times V_{Injected}\times V_{Sample}}, \quad (1)$$

in which V_{Sample} is the sample volume (mL) of the algal solution; $V_{Injected}$, the volume of pigment extract injected into the chromatographic column; l, the optical path-length of the HPLC flow cell, which is 1 cm in this study, and n is the pigment types detected by HPLC. The 14 main pigments measured in the Yellow/East China Sea waters are chlorophyll *a* (Chl *a*), chlorophyll *b* (Chl *b*), chlorophyll *c* (Chl *c*), the photosynthetic carotenoids (PSC) peridinin, 19'-But., Fuco., and β.ε-Car., and the photoprotective carotenoids (PPC) Neo., Viola., Diadino., Allo., Pras., Zea., and β.β-Car. They are divided into the five main groups of pigments (Chl *a*, Chl *b*, Chl *c*, PSC, and PPC).

2.2 Absorption coefficient spectral decomposition

2.2.1 Gaussian decomposition

Empirical evidence derived using the Gaussian method to decompose the spectra of chlorophyll and chlorophyll-protein complex absorption in solution shows that Gaussian curves can express independent absorption bands of pigments. Hoepffner and Sathyendranath (1991) suggested that $a_{\mathrm{ph}}(\lambda)$ can be modeled by accumulating 13 Gaussian bands. Under unpackaged conditions, the relationship between the phytoplankton specific absorption coefficient $a^*_{\mathrm{ph}}(\lambda)$ and pigment concentration can be expressed as follows, with the help of the Gaussian band decomposition of absorption coefficient spectra of the separated pigment components:

$$a_{\mathrm{ph}}(\lambda) = Q^*(\lambda) \times \sum_{i=1}^{n} C_i \sum_{j=1}^{L} a^*_j(\lambda_{mj}) e^{-\frac{1}{2}\left(\frac{\lambda-\lambda_{mj}}{\sigma_{ij}}\right)^2}, \quad (2)$$

in which, $Q^*(\lambda)$ (dimensionless) is the spectral function of pigment package effect factor; C_i the concentration of the i^{th} pigment of n total pigments, a^*_j is the pigment-specific absorption coefficient of the j^{th} extreme value in the λ_{mj} band of L total bands, λ_{mj} is the j^{th} extreme band of the Gaussian band, and σ_{ij} is the half-wave width of the Gaussian band.

In this study, we use the Hoepffner and Sathyendranath (1991) model and the Chase et al. (2013) model to decompose phytoplankton absorption spectra into 13 bands. Because Case II water (Morel and Prieur (1977) is defined in which all components vary with chlorophyll (Case I) to those where it is not the case (Case II), such as open ocean vs. coastal water) often has small absorption values at near infrared wavelengths (λ>700 nm), the 700-nm reference central wavelength and 15-nm half-wave width are added into the Chase model (originally 12 bands) by referring to the Hoepffner model design. French et al. (1972) reported that the decomposition of chlorophyll *a* in the infrared band could also produce a similar Gaussian component band at 700–706 nm.

2.2.2 Component pigment spectral analysis

Using pigment-specific spectra (rather than Gaussian method) is another potential method for estimating phytoplankton pigments from absorption spectra. The unknown phytoplankton absorption spectra can be decomposed using known in vivo pigment specific absorption coefficients obtained from measurements of extracted pigments. The empirical coefficient of pigment decomposition is as follows:

$$a^*_{\mathrm{ph}}(\lambda) = \frac{1}{C_a} \sum [a^*_j(\lambda) C_j], \quad (3)$$

$$a^*_j(\lambda) = \sum a^*_{\mathrm{max},i} e^{-\frac{1}{2}\left(\frac{\lambda-\lambda_{\mathrm{max},i}}{\sigma_i}\right)^2}, \quad (4)$$

where j is the pigment group index (j=Chl *a*, Chl *b*, Chl *c*, photosynthetic carotenoids (PSC), photoprotective carotenoids (PPC), unidentified pigments (UP) such as phycobilins that cannot be measured by HPLC); $a^*_j(\lambda)$ [m^2/(mg pigment)] is the spectral mass-specific absorption coefficient of the j^{th} pigment in unpackaged conditions; C_j [m^2/(mg pigment)] is the concentration of the j^{th} pigment group (i.e. *a*, *b*, *c*, PSC, PPC, UP); $a^*_{\mathrm{max},i}$ [m^2/(mg pigment)] is the mass-specific absorption coefficient for the peak of the Gaussian band; $\lambda_{\mathrm{max},i}$ [nm] is the central wavelength of the band; and σ_i [nm] is the half-wave width of the Gaussian band.

The specific absorption coefficient curves of different model components include: 1) the marine algorithm defined by Woźniak et al. (2000), with which the basic Gaussian absorption bands of pigments can be separated from each other; 2) the Baltic Sea algorithm constructed by Ficek et al. (2004) that includes UP components; 3) the Gaussian bands decomposed by the Hoepffner and Sathyendranath (1991) model, which can also perform classification based on pigment composition into four major groups: Chl *a*, Chl *b*, Chl *c*, and carotenoids (Carot.); and 4) the Bidigare et al. (1990) model, which yields directly the absorption coefficients for the five major pigment components.

2.3 Correction of pigment package effect

The package effect of pigments results in a reduction in the in vivo absorption coefficient of every unit of pigment concentration in phytoplankton due to package self-shielding effects in pigmented cells. Before using a mathematical formula (algorithm) to describe the relationship between the phytoplankton absorption coefficient and the pigment concentration function, the package effect on the observed phytoplankton absorption coefficient must be eliminated or reduced (Morel and Bricaud, 1981). The relationship between the in vivo phytoplankton spectrum absorption coefficient $a_{\mathrm{ph}}(\lambda)$, the in vivo algal specific absorption coefficient spectrum $a^*_{\mathrm{ph}}(\lambda)$,

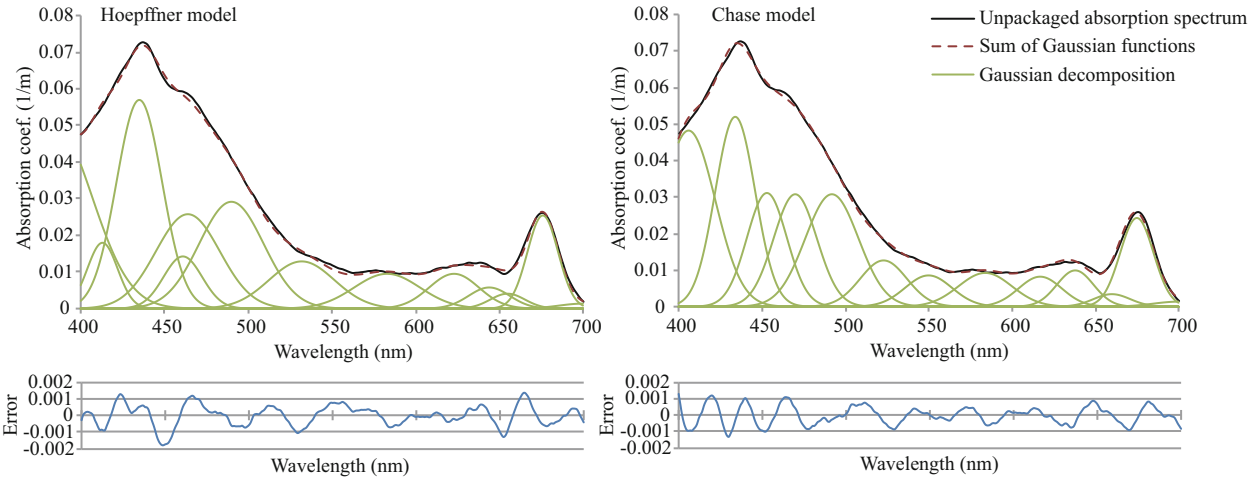

Fig.2 Absorption spectra corrected for the package effect (black line, e.g. HD04_10) and the corresponding fitted spectra (red dashed line), expressed as the sum of 13 Gaussian components (green line); the error curve (the difference between the observed and fitted curves) is shown in the lower panel (blue line)

and the phytoplankton pigment specific absorption coefficient spectrum in the in solvent state $a^*_{ph,s}(\lambda)$ can be expressed in a simplified form as follows (Bricaud et al., 1995; Woźniak et al., 2000):

$$a_{ph}(\lambda)=a^*_{ph}(\lambda)\times C_a, \quad (5)$$

$$a^*_{ph}(\lambda)=Q^*(\lambda)\times a^*_{ph,s}(\lambda). \quad (6)$$

The spectral function of the pigment package effect can be expressed as follows (Van De Hulst, 1957; Morel and Bricaud, 1981):

$$Q^*(\lambda)=\frac{3}{2\rho'(\lambda)}\left[1+\frac{2e^{-\rho'(\lambda)}}{\rho'(\lambda)}+2\frac{e^{-\rho'(\lambda)}-1}{(\rho'(\lambda))^2}\right], \quad (7)$$

$$\rho'(\lambda)=a^*_{ph,s}(\lambda)\times C_I\times d, \quad (8)$$

in which the subscript s indicates dissolved conditions; $a^*_{ph}(\lambda)$ [m^2/(mg tot. Chl *a*)] is the phytoplankton total specific absorption coefficient; $a^*_{ph,s}(\lambda)$ [m^2/(mg tot. Chl *a*)] is the phytoplankton pigment total absorption coefficient under dissolved conditions; C_a [(mg tot. Chl *a*)/m^3] is the chlorophyll *a* concentration in seawater; $Q^*(\lambda)$ [dimensionless] is the spectral function of pigment package effect factors; C_I [(mg tot. Chl *a*)/m^3] is the intracellular chlorophyll concentration, and *d* [m] is the cell diameter.

It should be noted that Eqs.5–8 focus on monotonic dispersion and uniformly spherical phytoplankton cells, making it applicable to a rational simplification for different phytoplankton species in natural waters (with different shapes and particle sizes, or complex, non-uniform internal structures) (Morel and Bricaud, 1981; Sathyendranath et al., 1987; Nelson and Prézelin, 1990). In practice (Ficek et al., 2004), when focusing on a certain natural species of phytoplankton, this equation is acceptable as long as $C_I\times d$ in Eq.8 is treated as equivalent to the approximate average width. Because the cell concentration and particle size of the Yellow Sea phytoplankton has not been directly measured, we calculated and calibrated the package effect by referring to the Baltic Sea model by Ficek et al. (2004), which is coastal Case II water and has similar optical properties to the Yellow/East China Sea study area, to calculate $C_I\times d$ and the specific absorption coefficients $a^*_{ph,s}$ of algal species:

$$C_I\times d=10.77C_a^{0.3767}. \quad (9)$$

3 RESULT

3.1 Gaussian band decomposition of absorption spectra under unpackaged conditions

The two slightly different Gaussian decomposition results (Fig.2) indicate that Gaussian decomposition of different characteristic bands and half-wave widths fitted well to different phytoplankton absorption curves after package effect correction. In addition, the residual error was small, with most bands within ±0.001 (1/m) in all stations. The central wavelengths and half-wave widths of the 13 bands may change in different phytoplankton species or different physiological stages of photosynthesis (for example, a change in the ratio of photosystem I (PS I) to photosystem II (PS II) should induce a slight variation in the wavelength position of the Chl *a* absorption maximum) (Hoepffner and Sathyendranath, 1991). In this study, a fixed characteristic band decomposition is used instead of station-by-station adjustment to avoid a large residual error (>0.001 (1/m)) in some feature bands.

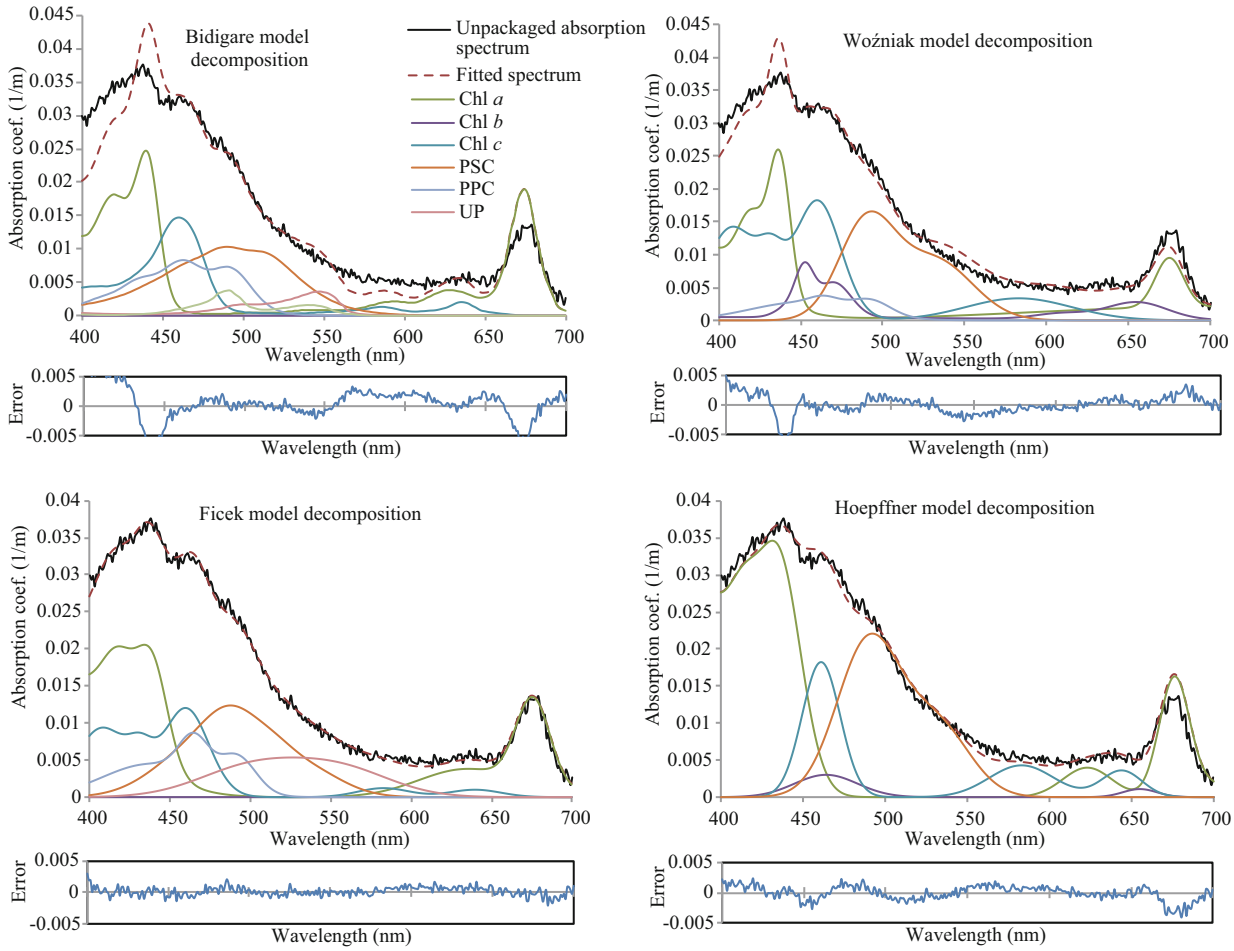

Fig.3 Absorption spectra corrected for the package effect (black line, e.g. HD04_1) and the corresponding fitted spectra (red dashed line), expressed as the sum of pigment components (Chl *a*, Chl *b*, Chl *c*, PSC, PPC, UP) from the Bidigare, Woźniak, Ficek, and Hoepffner models; the error curve is shown in the lower panel (blue line)

3.2 Pigment decomposition of absorption spectra

The non-negative least squares method used in the Bidigare et al. (1990), Woźniak et al. (2000), Ficek et al. (2004), and Hoepffner and Sathyendranath (1991) models are used for multiple regression decomposition of phytoplankton absorption spectra (Fig.3, using station HD04_1 as an example). The four methods can decompose the original spectra well for most bands. The Bidigare and Woźniak spectrum decomposition models overestimated clearly the 440 nm chlorophyll *a* absorption peak with a relatively large residual error. The Bidigare spectrum decomposition model clearly underestimated at 400–430 nm and overestimated at 676 nm, and the goodness of fitting is the lowest among the four models. There is a very small residual error in the decomposition of phytoplankton absorption spectrum using the non-negative least squares method in the Ficek model, in which the error in most bands is <0.001 (1/m); thus, it is the closest to the "true values", and the Hoepffner model has the second lowest residual error. Comparing the spectrum decomposition results among all stations, the Ficek decomposition model generated the smallest residual error in the absorption spectrum and was the closest to the "true values", whereas the Bidigare decomposition model had the largest residual error. To determine whether a decomposition model of the pigment composition curve fits the absorption spectrum characteristics in a station, the pigment composition specific absorption spectra and decomposition coefficients (corresponding to pigment concentration) are important factors influencing the size of the residual errors during construction of the curve.

3.3 The relationship between Gaussian decomposition characteristic bands and pigment concentration

In the central band and half-wave widths of the

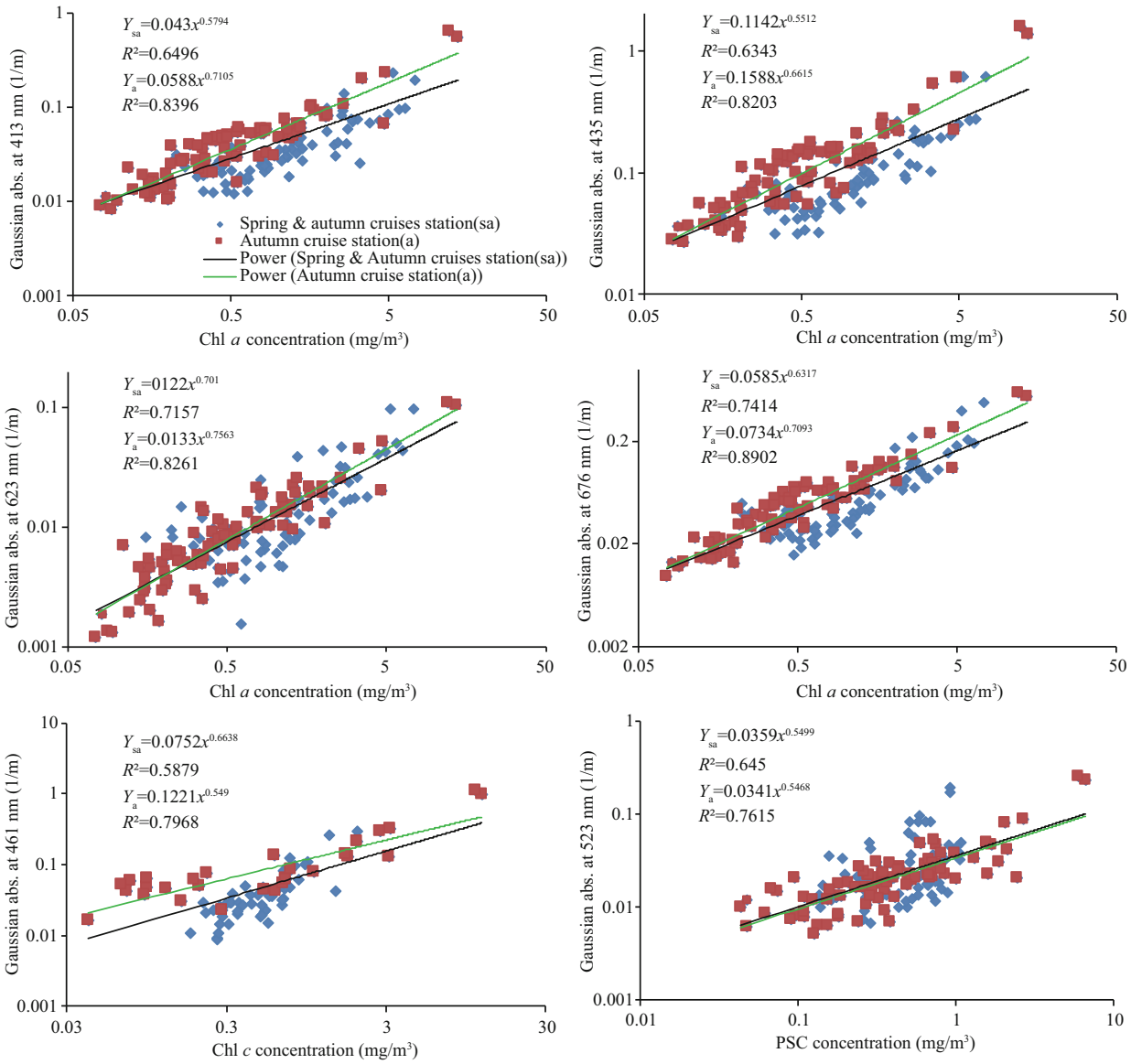

Fig.4 The band height of Hoepffner model Gaussian decomposition at 413 nm, 435 nm, 623 nm, and 676 nm vs. Chl *a* concentration, 461 nm vs. Chl *c* concentration, Chase model's 523 nm vs. PSC concentration

These pigment concentrations are measured by HPLC. Y_{sa} represents the fitting value of the spring and autumn cruises (black line), and Y_a the fitting value of the autumn cruise (green line).

Hoepffner and Sathyendranath (1991) Gaussian bands, all phytoplankton absorption spectrum curves under unpackaged conditions were decomposed into 13 Gaussian bands representing the absorption of the major pigments. The initial peak height of every band was adjusted based on the absorbance level at 440 nm. Under the effects of pigment composition and the pigment package, the relationship between phytoplankton absorption coefficient and pigment concentration could be discribed by multiple functional relationships (linear, quadratic polynomial, exponential, and hyperbolic functions). The power relationship between the absorption coefficient under unpackaged conditions and chlorophyll *a* ($Y=A[\text{Pigments}]^B$) is often used in observations of the natural environment (Bricaud et al., 1995, 1998; Chase et al., 2013, 2017; Wang et al., 2018).

A power regression was performed between the characteristic bands and pigment composition that measured by HPLC in 157 match-up sets (Fig.4). Overall, the regression goodness of individual cruises was high except for Chl *b* in the autumn cruise; the R^2 goodness of the characteristic bands was 0.65 or greater in the autumn cruise (Table 1). The overall trends of the two cruises are consistent but the regression goodness decreased. The regression

Table 1 Correlation between HPLC pigment concentration and band height in the Hoepffner model of the Gaussian decomposition in 12 different pigment absorption wavelengths

Wavelength (nm)	Pigment (s)	R^2	A	B	e_{median} (%)
413	Chl *a*	0.839 6	0.058 8	0.710 5	31
435	Chl *a*	0.820 3	0.155 8	0.661 5	36
623	Chl *a*	0.826 1	0.013 3	0.756 3	26
676	Chl *a*	0.890 2	0.073 4	0.709 3	25
464	Chl *b*	0.460 6	0.198 6	0.446 9	72
655	Chl *b*	0.488 5	0.017	0.488	88
461	Chl *c*	0.796 8	0.122 1	0.549	60
583	Chl *c*	0.703 5	0.025 6	0.307 4	85
644	Chl *c*	0.690 1	0.020 6	0.358	80
490	Carot.	0.721 6	0.161 5	0.614 2	44
532	Carot.	0.650 5	0.057 2	0.523 2	52
523[a]	PSC	0.761 5	0.034 1	0.546 8	40

Correlation values are the Pearson correlation coefficient (R^2). A and B are coefficients determined using $Y=A[\text{Pigment}_j]^B$ and $[\text{Pigment}_j]=(Y/A)^{(1/B)}$. Note that using type-I regression and error estimates as in $e_{median}=(\text{median}((\text{abs}([\text{Pigment}_j]-\text{HPLC}_j))/\text{HPLC}_j))\times 100$, where for 50% of the data, the error in pigment concentration prediction is less than the e_{median} value, it assumes HPLC to be error free (Chase et al., 2013). Caro t.=Neo.+Viola.+Diadino.+Allo.+Pras.+Zea.+β.β-Car; PSC=Peridinin+19'-But.+Fuco.+β.ε-Car; e_{median}: median relative error (%); [a]: the band was referenced from Chase et al. (2013).

goodness of Chl *b* characteristic band was low as the results at 464 nm and 655 nm were more dispersed. Chl *b* sample concentration obtained from HPLC measurements was also slightly lower than those of other pigment components. In addition, the degree of overlap in the absorption spectrum of Chl *b* with other pigments, especially Chl *a*, was high, and in low light conditions, the absorbance of Chl *b* was completely covered by Chl *a* (Hoepffner and Sathyendranath, 1991). The regression goodness of Chl *c* characteristic bands was relatively high compared to Chl *b* but its median relative errors (e_{median} (%)) were a little bigger. The concentration of carotenoid was generally scattered at 490 nm and 532 nm in the Gaussian decomposition band height, which may be related to unmeasured pigment components. The Gaussian decomposition bands in the Chase model showed the same trend as the Hoepffner model, and the R^2 goodness of fit of PSC characteristic band was acceptable as the median relative error (e_{median} (%)) was small (Table 1).

The 676-nm band represents the primary absorbance of Chl *a*, and the R^2 values of the correlation were the highest among Chl *a* absorption bands, and the next highest was in the 413 nm band. The distribution of data points shows that data from the spring and autumn cruises in 2003 overlapped the most at the 623 nm band (high overlap between autumn and spring regression curves) shown in Fig.4. Correction of the pigment package effect presented that the bands near 623 nm were corrected the least, meaning that the absorption coefficients were minimally affected by the package effect. This conclusion is consistent with a study by Stuart et al. (1998) suggesting that the package effect at the 623 nm band is small enough to be ignored. The relationship between peak height and pigment concentration is virtually unaffected by phytoplankton species type. If the package effect were not fully corrected, the results among different species would be more scattered. Each characteristic band is somewhat affected by the collective effect of absorption of other pigment components, which is also a key reason for the poor correlation between characteristic bands and their corresponding pigments (Chase et al., 2013).

3.4 Relationship between model-based pigment concentration and HPLC-based pigment concentration

The Ficek model showed a good fit as indicated by the relationship between its non-negative least-square decomposition of phytoplankton absorption spectra composition and HPLC-measured pigment concentration. As shown in Fig.5, except for the slightly higher concentration of Chl *a* in autumn (red squares), all the other pigments distributed near the 1:1 line. This may be related to samples being collected in different water seasons or the Ficek model includes the contribution of unidentified pigments (UP). Closeness to the 1:1 line indicates the basic suitability of the decomposition method, and supports indirectly the rationality of the spectrum model for pigment decomposition. Among the five main groups of components, Chl *a* and Chl *c* showed relatively good fitting, whereas Chl *b* was relatively scattered. The autumn cruise showed very poor fitting, nearly no correlation, which is consistent with the Gauss decomposition results. Overall, the degree of fit of individual cruises was high (R^2=0.9 or greater) especially for Chl *a* and Chl *c* in the autumn cruise. The Woźniak model showed a better fit than the Ficek model for Chl *a* concentration and nearest to the 1:1 line except for an offset point (Fig.5), and the median relative error (e_{median} (%)) was low (Table 2). The two

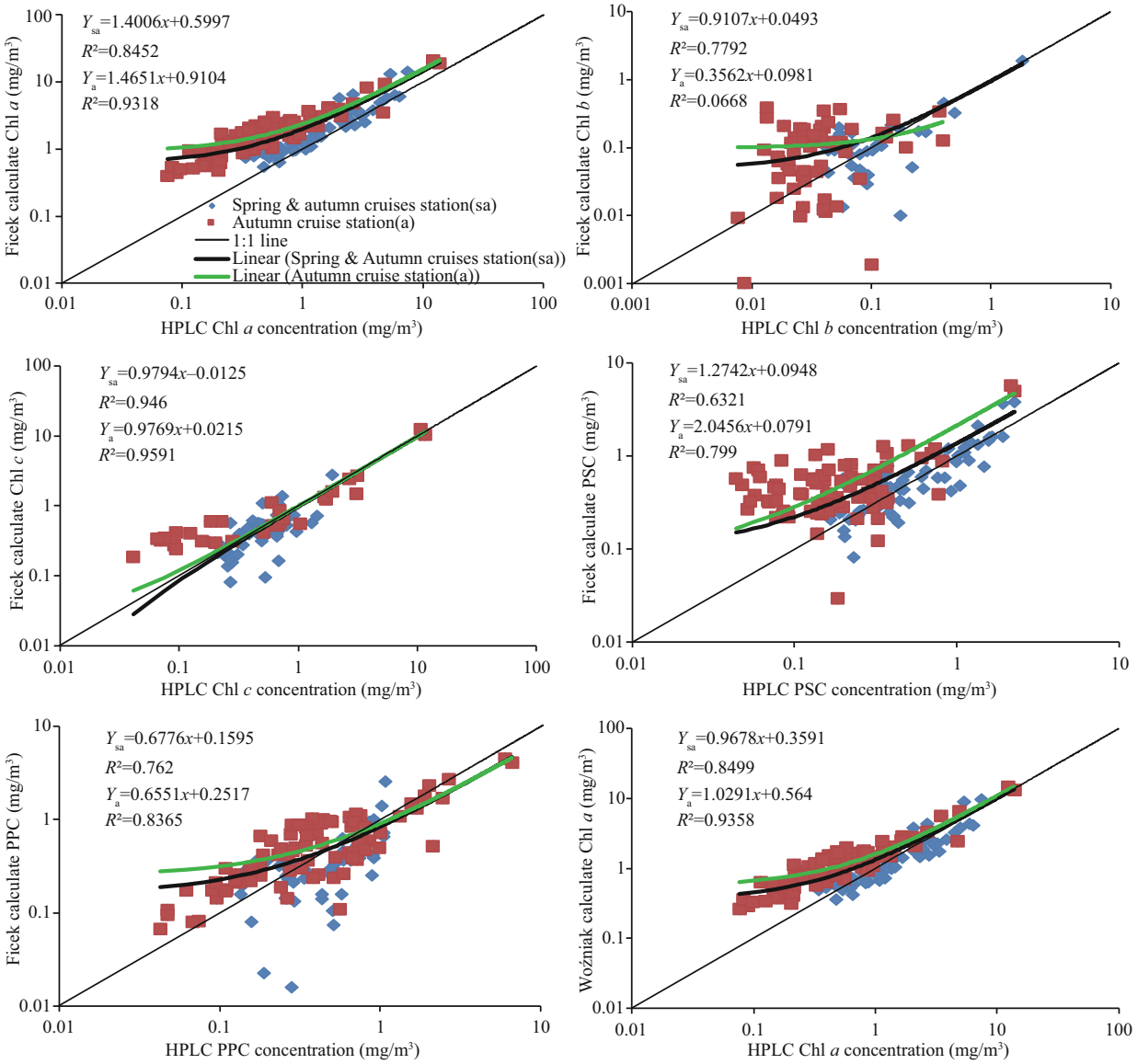

Fig.5 Pigment composition decomposed from unpackaged absorption spectra using the Ficek model vs. pigment concentration, Woźniak model vs. Chl *a* concentration

These pigments concentrations are measured in HPLC. Formula Y_{sa} represents the value of the spring and autumn cruises (black line), and Y_a represents the value of the autumn cruise (green line). The diagonal line is the 1:1 line.

Table 2 The median relative errors (e_{median} (%)) between HPLC pigment concentrations and pigment composition decomposed from unpackaged absorption spectra using different models

Error estimate	Pigment	Ficek model	Woźniak model	Bidigare model	Hoepffner model
Autumn e_{median} (%)	Chl *a*	134	61	285	225
	Chl *b*	76	683	109	1049
	Chl *c*	31	44	53	104
	PPC	84	219	102	380
	PSC	44	46	69	/
Spring e_{median} (%)	Chl *a*	50	28	140	101
	Chl *b*	49	208	61	351
	Chl *c*	29	38	46	102
	PPC	27	114	49	193
	PSC	36	40	41	/

Note that using type-I regression and error estimates as in e_{median}=(median ((abs ([Pigment$_i$]−HPLC$_i$))/HPLC$_i$))×100, where for 50% of the data, the error in pigment concentration prediction is less than the e_{median} value, it assumes HPLC to be error free. / means no data.

cruises had overall similar trends, but the degree of fit decreased slightly from spring to autumn (Table 2), which may be related to differences in the phytoplankton community structure.

4 DISCUSSION

4.1 Methodological uncertainties in field data measurements

The absorption coefficient of phytoplankton is a complex summation of absorption coefficients of photosynthetic carotenoid (PSC) and photo-protective carotenoid (PPC). Diverse results and conclusions can be drawn when different methods or classification criteria are applied. The methodological uncertainties in field data measurements could affect the results. Many available methods can determine that $a^*_{ph}(\lambda)$ is equal to $a^*_{ph,s}(\lambda)$, or the $a^*_{ph}(\lambda)$ in an organic solvent such as methanol, acetone, Triton-X, etc. Theoretically, $a^*_{ph,s}(\lambda)$ varies with the type of organic solvent; for examples, it is 0.020 2 m^2/[mg Chl *a*] at 664 nm in 90% acetone or 0.017 1 m^2/[mg Chl *a*] at 665 nm in methanol (Bissett et al., 1997). The absorption coefficients of pigments measured by the HPLC would be significantly larger than the QFT, in vivo phytoplankton measurement (InVivo), and acetone extracts pigments measurement (AceEx) methods (Zhu et al., 2017), and the QFT and InVivo methods had obviously a package effect in the measurement of absorption coefficient. The pigment types and numbers detected by HPLC can also affect the results, and it would have a small difference measured more or less than 14 main pigments in the Yellow/East China Seas waters.

4.2 Environmental uncertainties in field data measurements

The environmental uncertainties in irradiance and nutrients in field data measurements would affect the results. The pigment content per cell varies with these environmental factors even within a particular class. The change in the nutrient regime affects the internal accumulation of pigments and their packaging degree, and could induce physiological responses of the existing phytoplankton communities (Allali et al., 1997). Normally, there exists a strong thermal stratification phenomenon (~5°C) between the 5 to 10 m depths in the Yellow/East China Sea. The two season datasets are different from each other in depth, which is 10–20 m in spring and 0–5 m in autumn. Thus, the spring cruise data from deeper depths cannot be considered as "surface" data. The autumn cruise data, the water column that is well mixed and considered as "surface" data. It can be applicable to estimate chlorophylls *a*, *b*, *c*, the photosynthetic carotenoids, and the photoprotective carotenoids using hyperspectral reflectance from in-situ device or satellite image in Yellow/East China Seas in the future. However, it is meaningful to analyze the effect of Gaussian decomposition and the component pigment absorption spectra of phytoplankton in different seasons and depths in a same area. Phytoplankton at different depths is always of different species and sizes in the phytoplankton community structure, so the package effect is very changeable to test the stability of the model.

4.3 The capability of detection to various pigments

Strong correlations were observed when comparing two major chlorophyll pigments (chlorophylls *a*, and *c*), PSC, and carotenoid pigment in peak absorption wavelength for each pigment except for chlorophylls *b* in the Yellow/East China Sea (Fig.4, Table 1). The median relative errors (e_{median} (%)) ranged 25%–52% for chlorophyll *a*, PSC, and carotenoid pigment, and 60%–85% for chlorophyll *c* (Table 1). Other uncertainty factors may include unmeasured pigment components, such as chlorophyll *c*3 and other accessory matters. There is a tiny peak-location shift of 1–6 nm in the characteristic bands in the Gaussian decomposition between Chase model and Hoepffner model but it is too small to affect the correlation in band height between HPLC pigment concentration and Hoepffner/Chase model in the Gaussian decomposition. The R^2 value is acceptable between PSC pigment concentration and Chase model's characteristic band height at 523 nm, and the median relative error (e_{median} (%)) is small (Table 1). We determined a strong capability for predicting chlorophylls *a*, *c*, carotenoids, and PSC. The weak correlation between Gaussian decomposition characteristic band height (464 nm and 655 nm) and chlorophyll *b* concentration may be attributed to the unmeasured accessory pigment components such as divinyl Chl *b*, Chl *b* epimers, etc.

Given that it is expensive and time consuming to measure all the necessary pigments and collect good quality data in the field, a potentially alternative method for estimating phytoplankton pigments from absorption spectra is to use pigment-specific spectra. The Fieck model worked well in deep water samples

in the spring cruise for all the five major pigment components but it deviates from the 1:1 line for surface water samples of the autumn cruise. More work is called to tune the model and achieve a good fit of variable relationships between absorption spectra and pigment concentrations in the coastal sea. Compared with the Ficek model, the Woźniak model showed a better fit for Chl *a* concentration and is the nearest to the 1:1 line. The possible presence of Chl *b* or divinyl Chl *b* and other accessory pigments are a minimal influence to the red absorption band of Chl *a* at 675 nm (Fig.3), as Bricaud et al. (1995) corrected for the enhancement in this case by measuring the height of the band above the baseline where $a^*_{ph}(660)$ and $a^*_{ph}(700)$ joins.

Pigment component information estimated from phytoplankton absorption spectra helps better remote sensing of hyperspectral color change in the ocean that related to the changes in phytoplankton community varieties. Many previous studies of detecting phytoplankton groups and pigments are conducted using multispectral reflectance data and/or are developed for a specific region (Werdell et al., 2014; Bracher et al., 2015, 2017) or the global ocean (Chase et al., 2017; Wang et al., 2018) belonged to the Case I water. In the future, we will use hyperspectral reflectance from in-situ radiometers or satellite images in Case II water of the Yellow/East China Sea.

5 CONCLUSION

Employing phytoplankton absorption coefficient spectra and pigment concentration as the base, we combined non-negative least-square analysis with the characteristic band information of major component pigment absorption spectrum and a basic empirical model of the specific absorption coefficients of five main groups of algal pigments (Chl *a*, Chl *b*, Chl *c*, PSC, and PPC) to conduct a Gaussian decomposition and pigment empirical decomposition from the absorption spectra of phytoplankton from the Yellow/East China Sea in 2003 under unpackaged conditions.

With respect to absorption coefficient spectra decomposition, 13 characteristic bands from the Gaussian decomposition using the Hoepffner and Chase models are decomposed effectively from the spectra from all stations. Good results were achieved even if fixed characteristic bands were used, and the residual error in the vast majority of bands had an absolute value of less than 0.001 (1/m). Our power regression analysis showed that the 623 nm band that affected least by the package effect had the highest regression overlap between the spring and autumn cruises in 2003. Overall, the regression for individual cruises was better than that for the two cruises combined, especially for the autumn cruise (except for Chl *b*), in which the R^2 of the power regression for characteristic bands was 0.65 or higher. Our method showed a strong capability of detection to chlorophylls *a*, *c*, carotenoids, and PSC. In addition, estimation of pigment concentration from empirical specific absorption coefficient of pigment composition in the Bidigare, Woźniak, Ficek, and Hoepffner non-negative least-square models is tested, applied, and compared for all the Yellow/East China Sea data in 2003. The Ficek model agreed well with the HPLC measurement data, by which most data points are distributed near the 1:1 line; however, a seasonal bias is apparent. The Woźniak model worked better than the Ficek model for Chl *a*, showing a smaller median relative error.

Because changes in absorption spectrum are affected by many factors such as the package effect, measurement technique, water environment, and algal species, in the future, it is necessary to develop a pigment component absorption model for Chinese offshore waters to increase the decomposition accuracy for different times, areas, and algal species.

6 DATA AVAILABILITY STATEMENT

The data of this study are available from the China's National Ocean Technology Center but restrictions may apply due to the availability of some of the data that were used under license for this study, and thus, they are not publicly available. The data are however available from the authors upon reasonable request and with permission from the National Ocean Technology Center.

7 ACKNOWLEDGEMENT

We are grateful to the experimental crews of cruises in April 2003 spring and September 2003 autumn Yellow/East China Sea for their hard work during water sample collection, measurement, and analysis. The authors also thank the two anonymous reviewers for their insightful comments, which helped greatly in improving the manuscript.

References

Allali K, Bricaud A, Claustre H. 1997. Spatial variations in the chlorophyll-specific absorption coefficients of phytoplankton and photosynthetically active pigments in the equatorial

Pacific. *Journal of Geophysical Research*: *Oceans*, **102**(C6): 12 413-12 423, https://doi.org/10.1029/97JC00380.

Bidigare R R, Morrow J H, Kiefer D A. 1989. Derivative analysis of spectral absorption by photosynthetic pigments in the Western Sargasso Sea. *Journal of Marine Research*, **47**(2): 323-341, https://doi.org/10.1357/002224089785076325.

Bidigare R R, Ondrusek M E, Morrow J H, Kiefer D A. 1990. In-vivo absorption properties of algal pigments. *In*: Proceedings of SPIE 1302, Ocean Optics X. SPIE, Orlando. p.290-302, https://doi.org/10.1117/12.21451.

Bissett W P, Patch J S, Carder K L, Lee Z P. 1997. Pigment packaging and Chl *a*-specific absorption in high-light oceanic waters. *Limnology and Oceanography*, **42**(2): 961-968, https://doi.org/10.4319/lo.1997.42.5.0961.

Bracher A, Bouman H A, Brewin R J W, Bricaud A, Brotas V, Ciotti A M, Clementson L, Devred E, Di Cicco A, Dutkiewicz S, Hardman-Mountford N J, Hickman A E, Hieronymi M, Hirata T, Losa S N, Mouw C B, Organelli E, Raitsos D E, Uitz J, Vogt M, Wolanin A. 2017. Obtaining phytoplankton diversity from ocean color: a scientific roadmap for future development. *Frontiers in Marine Science*, **4**: 55, https://doi.org/10.3389/fmars.2017.00055.

Bracher A, Taylor M H, Taylor B, Dinter T, Röttgers R, Steinmetz F. 2015. Using empirical orthogonal functions derived from remote-sensing reflectance for the prediction of phytoplankton pigment concentrations. *Ocean Science*, **11**(1): 139-158, https://doi.org/10.5194/os-11-139-2015.

Bricaud A, Babin M, Morel A, Claustre H. 1995. Variability in the chlorophyll-specific absorption coefficients of natural phytoplankton: analysis and parameterization. *Journal of Geophysical Research*: *Oceans*, **100**(C7): 13 321-13 332, https://doi.org/10.1029/95JC00463.

Bricaud A, Claustre H, Ras J, Oubelkheir K. 2004. Natural variability of phytoplanktonic absorption in oceanic waters: influence of the size structure of algal populations. *Journal of Geophysical Research*: *Oceans*, **109**(C11): C11010, https://doi.org/10.1029/2004JC002419.

Bricaud A, Mejia C, Blondeau-Patissier D, Claustre H, Crepon M, Thiria S. 2007. Retrieval of pigment concentrations and size structure of algal populations from their absorption spectra using multilayered perceptrons. *Applied Optics*, **46**(8): 1 251-1 260, https://doi.org/10.1364/AO.46.001251.

Bricaud A, Morel A, Babin M, Allali K, Claustre H. 1998. Variations of light absorption by suspended particles with chlorophyll a concentration in oceanic (Case 1) waters: analysis and implications for bio-optical models. *Journal of Geophysical Research*: *Oceans*, **103**(C13): 31 033-31 044, https://doi.org/10.1029/98JC02712.

Chase A P, Boss E, Cetinić I, Slade W. 2017. Estimation of phytoplankton accessory pigments from hyperspectral reflectance spectra: toward a global algorithm. *Journal of Geophysical Research*: *Oceans*, **122**(12): 9 725-9 743, https://doi.org/10.1002/2017JC012859.

Chase A, Boss E, Zaneveld R, Bricaud A, Claustre H, Ras J, Dall'Olmo G, Westberry T K. 2013. Decomposition of in situ particulate absorption Spectra. *Methods in Oceanography*, **7**: 110-124, https://doi.org/10.1016/j.mio.2014.02.002.

Ferreira A, Ciotti Á M, Mendes C R B, Uitz J, Bricaud A. 2017. Phytoplankton light absorption and the package effect in relation to photosynthetic and photoprotective pigments in the northern tip of Antarctic Peninsula. *Journal of Geophysical Research*: *Oceans*, **122**(9): 7 344-7 363, https://doi.org/10.1002/2017JC012964.

Ficek D, Kaczmarek S, Stoń-Egiert J, Woźniak B, Majchrowski R, Dera J. 2004. Spectra of light absorption by phytoplankton pigments in the Baltic; conclusions to be drawn from a Gaussian analysis of empirical data. *Oceanologia*, **46**: 533-555.

French C S, Brown J S, Lawrence M C. 1972. Four universal forms of chlorophyll a. *Plant Physiology*, **49**(3): 421-429.

Hoepffner N, Sathyendranath S. 1991. Effect of pigment composition on absorption properties of phytoplankton. *Marine Ecology Progress Series*, **73**: 11-23, https://doi.org/10.3354/meps073011.

Le C F, Li Y M, Zha Y, Sun D Y. 2009. Specific absorption coefficient and the phytoplankton package effect in Lake Taihu, China. *Hydrobiologia*, **619**(1): 27-37, https://doi.org/10.1007/s10750-008-9579-6.

Lee Z P, Carder K L. 2004. Absorption spectrum of phytoplankton pigments derived from hyperspectral remote-sensing reflectance. *Remote Sensing of Environment*, **89**(3): 361-368, https://doi.org/10.1016/j.rse.2003.10.013.

Mitchell B G. 1990. Algorithms for determining the absorption coefficient for aquatic particulates using the quantitative filter technique. *In*: Proceedings of SPIE 1302, Ocean Optics X. SPIE, Orlando. p.137-148, https://doi.org/10.1117/12.21440.

Morel A, Bricaud A. 1981. Theoretical results concerning light absorption in a discrete medium, and application to specific absorption of phytoplankton. *Deep Sea Research Part A*. *Oceanographic Research Papers*, **28**(11): 1 375-1 393, https://doi.org/10.1016/0198-0149(81)90039-X.

Morel A, Prieur L. 1977. Analysis of variations in ocean color. *Limnology and Oceanography*, **22**(4): 709-722, https://doi.org/10.4319/lo.1977.22.4.0709.

Nelson N B, Prézelin B B. 1990. Chromatic light effects and physiological modeling of absorption properties of *Heterocapsa pygmaea* (=*Glenodinium* sp.). *Marine Ecology Progress Series*, **63**: 37-46, https://doi.org/10.3354/meps063037.

Pegau S, Zaneveld J R V, Mueller J L. 2003. Inherent optical property measurement concepts: physical principles and instruments. *In*: Mueller J L, Fargion G S, McClain C R eds. NASA/TM 2003 Ocean Optics Protocols for Satellite Ocean Color Sensor Validation-Inherent Optical Properties: Instruments, Characterization, Field Measurements and Data Analysis Protocols. NASA, Washington, DC. p.1-64.

Sathyendranath S, Lazzara L, Prieur L. 1987. Variations in the spectral values of specific absorption of phytoplankton.

Limnology and Oceanography, **32**(2): 403-415, https://doi.org/10.4319/lo.1987.32.2.0403.

Stuart V, Sathyendranath S, Platt T, Maass H, Irwin B D. 1998. Pigments and species composition of natural phytoplankton populations: effect on the absorption spectra. *Journal of Plankton Research*, **20**(2): 187-217, https://doi.org/10.1093/plankt/20.2.187.

Van De Hulst H C. 1957. Light Scattering by Small Particles. The John Wiley & Sons Inc., New York. p.287.

Vijayan A K, Somayajula S A. 2014. Effect of accessory pigment composition on the absorption characteristics of dinoflagellate bloom in a coastal embayment. *Oceanologia*, **56**(1): 107-124, https://doi.org/10.5697/oc.56-1.107.

Wang G Q, Lee Z P, Mouw C B. 2018. Concentrations of multiple phytoplankton pigments in the global oceans obtained from satellite ocean color measurements with MERIS. *Applied Sciences*, **8**(12): 2 678, https://doi.org/10.3390/app8122678.

Werdell P J, Roesler C S, Goes J I. 2014. Discrimination of phytoplankton functional groups using an ocean reflectance inversion model. *Applied Optics*, **53**(22): 4 833-4 849, https://doi.org/10.1364/AO.53.004833

Woźniak B, Dera J, Ficek D, Majchrowski R, Kaczmarek S, Ostrowska M, Koblentz-Mishke O I. 2000. Model of the *in vivo* spectral absorption of algal pigments. Part 1: mathematical apparatus. *Oceanologia*, **42**(2): 177-190.

Zhou W, Cao W X, Wang G F, Liang S J, Zhao J, Sun Z H. 2010. Retrieval of pigment concentrations from the absorption spectra of phytoplankton by multilayered perceptrons. *Journal of Tropical Oceanography*, **29**(2): 46-51. (in Chinese with English abstract)

Zhu J H, Zhou H L, Han B, Li T J. 2017. Measurement and feature analysis of absorption spectra of four algal species. *Chinese Journal of Oceanology and Limnology*, **35**(2): 350-359, https://doi.org/10.1007/s00343-016-5321-9.

Zhu J H. 2003a. The key technique for measuring spectral absorption coefficient of Case II water with spectrophotometer. *Ocean Technology*, **22**(1): 34-39. (in Chinese with English abstract)

Zhu J H. 2003b. Measurement of the ocean phytoplankton pigments concentration by HPLC. *Journal of Ocean Technology*, **22**(1): 14-19. (in Chinese with English abstract)